Widespread Changes in the Posttranscriptional Landscape at the Drosophila Oocyte-to-Embryo Transition

Citation: Kronja, Iva, Bingbing Yuan, Stephen W. Eichhorn, Kristina Dzeyk, Jeroen Krijgsveld, David P. Bartel, and Terry L. Orr-Weaver. "Widespread Changes in the Posttranscriptional Landscape at the Drosophila Oocyte-to-Embryo Transition." Cell Reports 7, no. 5 (June 2014): 1495–1508.

As Published: http://dx.doi.org/10.1016/j.celrep.2014.05.002

Publisher: Elsevier

Persistent URL: http://hdl.handle.net/1721.1/96184

Version: Final published version: final published article, as it appeared in a journal, conference proceedings, or other formally published context

Cell Reports
Article

Widespread Changes in the Posttranscriptional Landscape at the *Drosophila* Oocyte-to-Embryo Transition

Iva Kronja,[1] Bingbing Yuan,[1] Stephen W. Eichhorn,[1,2,3] Kristina Dzeyk,[4] Jeroen Krijgsveld,[4] David P. Bartel,[1,2,3] and Terry L. Orr-Weaver[1,2,*]
[1]Whitehead Institute, Cambridge, MA 02142, USA
[2]Department of Biology, Massachusetts Institute of Technology, Cambridge, MA 02142, USA
[3]Howard Hughes Medical Institute, Massachusetts Institute of Technology, Cambridge, MA 02142, USA
[4]European Molecular Biology Laboratory, 69117 Heidelberg, Germany
*Correspondence: weaver@wi.mit.edu
http://dx.doi.org/10.1016/j.celrep.2014.05.002

SUMMARY

The oocyte-to-embryo transition marks the onset of development. The initial phase of this profound change from the differentiated oocyte to the totipotent embryo occurs in the absence of both transcription and mRNA degradation. Here we combine global polysome profiling, ribosome-footprint profiling, and quantitative mass spectrometry in a comprehensive approach to delineate the translational and proteomic changes that occur during this important transition in *Drosophila*. Our results show that PNG kinase is a critical regulator of the extensive changes in the translatome, acting uniquely at this developmental window. Analysis of the proteome in *png* mutants provided insights into the contributions of translation to changes in protein levels, revealing a compensatory dynamic between translation and protein turnover during proteome remodeling at the return to totipotency. The proteome changes additionally suggested regulators of meiosis and early embryogenesis, including the conserved H3K4 demethylase LID, which we demonstrated is required during this period despite transcriptional inactivity.

INTRODUCTION

The oocyte-to-embryo transition marks the onset of development for any multicellular organism. This dramatic change involves the completion of meiosis in the oocyte, sperm entry, fusion of the male and female pronucleus, and the start of mitotic divisions (Horner and Wolfner, 2008b). These events accompany the profound developmental change from a differentiated oocyte into a totipotent embryo.

Studies on the restoration of cell potency have focused on the regulation of transcription (Young, 2011), but the oocyte-to-embryo transition necessitates a fundamentally different control mechanism. Following the primary arrest in prophase I, oocytes are transcriptionally silent, and in all animals at least the first embryonic division occurs prior to the initiation of zygotic transcription (Tadros and Lipshitz, 2009). Organisms such as insects, fish, and amphibians rely on stockpiled maternal mRNAs. These organisms proceed through several hours of embryonic development (i.e., 12–13 division cycles in *Xenopus* and *Drosophila*) prior to the onset of zygotic transcription, which also triggers turnover of maternal mRNAs (Anderson and Lengyel, 1979; Zalokar, 1976). In *Drosophila*, a pathway to degrade maternal mRNAs is not active until 2 hr after egg laying (Tadros et al., 2003, 2007). Thus, the oocyte-to-embryo transition and early embryogenesis occur with constant mRNA levels (Tadros and Lipshitz, 2009).

Although many aspects of translational regulation in the oocyte-to-embryo transition remain to be elucidated, the effect of translation on meiotic progression has been extensively analyzed in two other developmental contexts: (1) in yeast meiosis, which proceeds without developmentally programmed arrests and in the presence of transcriptional control, extensive translational regulation nevertheless occurs (Brar et al., 2012; Carlile and Amon, 2008; Chu and Herskowitz, 1998), and (2) in metazoans, at maturation the oocyte exits the primary arrest in prophase I and progresses into meiotic divisions. Experiments in amphibians, mice, and marine invertebrates demonstrated a role for cytoplasmic polyadenylation in activating translation at oocyte maturation and showed that precisely timed translation of several mRNAs is required for progression through the meiotic divisions (Charlesworth et al., 2013; Chen et al., 2011; Gebauer et al., 1994; Tay et al., 2000).

Here, we define the regulatory steps of gene expression at the oocyte-to-embryo transition of *Drosophila*. In *Drosophila*, as in most animals, the mature oocyte is arrested at a secondary point in meiosis (Sagata, 1996). In insects, this arrest point is the metaphase of meiosis I. The trigger for the oocyte-to-embryo transition is egg activation. Egg activation and exit from meiosis in *Drosophila* take place as the oocyte passes into the uterus, regardless of whether it is fertilized. Instead of sperm entry, mechanical pressure as well as osmotic and Ca^{2+} changes are thought to initiate egg activation in *Drosophila* (Horner and Wolfner, 2008a).

Egg activation is presumably accompanied by changes in translation, as poly(A) tails on mRNAs are lengthened and proteins involved in developmental patterning and cell-cycle control are synthesized (Horner and Wolfner, 2008b). In addition, proteins are actively subjected to degradation during egg activation. Release of the metaphase I arrest and completion of meiosis requires the Anaphase Promoting Complex/Cyclosome (APC/C) to target Cyclin B for degradation (Pesin and Orr-Weaver, 2007; Swan and Schüpbach, 2007). We recently showed that a meiosis-specific form of the APC/C also contributes to the change from meiosis in the oocyte to mitosis in the embryo by mediating degradation of the meiotic protein Matrimony (Mtrm) (Whitfield et al., 2013).

The *Drosophila* PNG kinase is required for the onset of mitotic divisions in the embryo (Fenger et al., 2000; Shamanski and Orr-Weaver, 1991). This Ser/Thr kinase is a complex of a catalytic subunit, encoded by the *png* gene, and two activating subunits, the proteins GNU and PLU (Lee et al., 2003). The PNG kinase complex is present and acts solely at the oocyte-to-embryo transition. By promoting the translation of *cyclin B* after egg activation, the PNG kinase complex leads to Cyclin B/Cdk1 reactivation and entry into the first embryonic mitosis (Fenger et al., 2000; Vardy and Orr-Weaver, 2007). PNG has an indirect role later in embryogenesis in promoting degradation of maternal mRNAs. This degradation requires Smaug (SMG), whose translation also is dependent on PNG at egg activation (Tadros et al., 2007).

We now quantitate changes in translation and the proteome that occur during the oocyte-to-embryo transition, a combined approach not previously used in any organism for this time frame, and identify regulators of this key developmental change. Our comprehensive approach allowed us to determine the extent to which translational changes are reflected in the proteome. These studies reveal that both extensive translational and posttranslational regulatory mechanisms sculpt the proteome at the developmental change from oocyte to embryo, and they emphasize the value of examining both the translatome and the proteome.

RESULTS

Translational Changes at Egg Activation

To assess globally the translational changes that occur at egg activation, we performed polysome profiling and ribosome footprinting of mature oocytes and activated eggs (Figure 1A). We used unfertilized *Drosophila* eggs instead of embryos because they undergo all the events of activation, including the completion of meiosis and the onset of expression of proteins that control embryonic patterning (Horner and Wolfner, 2008b). Unfertilized eggs offer an advantage over embryos: they allow monitoring of egg activation while avoiding the potentially confounding changes in protein synthesis and degradation that occur during the subsequent embryonic divisions of fertilized embryos.

In polysome profiling, mRNA-protein complexes are separated by fractionation through linear sucrose gradients (Beilharz and Preiss, 2004). The position of an mRNA within the sucrose gradient reflects its translational status: cosedimentation of mRNAs with ribonucleoproteins (RNPs) or ribosomal subunits suggests a lack of translation, whereas cosedimentation with polysomes indicates active translation. An abundant monosome peak present in the polysome profiles of mature oocytes was lost at egg activation, accompanied by a >5-fold gain in the relative abundance of polysomes (Figure 1B). To define the translational changes for each mRNA, we isolated mRNAs from six regions within the gradient (Figure 1B) and quantified their abundance by mRNA sequencing (mRNA-seq).

We identified 5,088 mRNAs (~35% of the annotated genes) in sucrose gradient fractions in two independent polysome-profiling experiments (Table S1). As expected, mRNA abundance in unfractionated lysates of mature oocytes and activated eggs, which are devoid of mRNA transcription and degradation, was highly correlated (R^2 = 0.89; Figure S1A). This result also indicated that although cytoplasmic polyadenylation has been reported to accompany egg activation, poly(A) selection is a reliable method for isolating mRNA in mature oocytes and activated eggs (Horner and Wolfner, 2008b; Sallés et al., 1994). Importantly, the mRNA abundance within the same fraction from two independent polysome-profiling experiments was highly correlated (R^2 = 0.72–0.99; Figures S1B and S1C), which allowed us to calculate the average percentage distribution of each mRNA across the six fractions.

To confirm that the mRNAs that cosedimented with the polysomal peaks (defined here as ≥5 ribosomes) were actively engaged in translation, we treated lysates of mature oocytes and activated eggs with puromycin ex vivo, which causes premature termination of elongating ribosomes (Blobel and Sabatini, 1971). The lysates were fractionated and mRNA-seq was performed. Puromycin treatment of mature oocytes and activated eggs was efficient, as it led to complete disassembly of polysomes as measured by OD_{254} (Figures S2A and S2B). Fractionation of puromycin-treated lysates of mature oocytes, but not of activated eggs, revealed that many mRNAs migrated within sucrose gradients in a translation-independent manner (Figures S2C and S2D). Following puromycin treatment of mature oocyte lysates, the median association of an mRNA with fractions corresponding to polysomes equaled a surprisingly high percentage of the total abundance (25%; Figure S2C). In contrast, in activated eggs after puromycin treatment, on average only 9% of the total mRNA cosedimented with the gradient regions corresponding to polysomes (Figure S2D). The large fraction of mRNA from mature oocytes that cosedimented, but was not actually associated with actively translating polysomes, highlights the necessity of the puromycin control in genome-wide polysome-profiling experiments. After correcting for translation-independent migration in the region corresponding to polysomes (see Supplemental Experimental Procedures), we classified 802 mRNAs as recruited onto polysomes, 729 mRNAs as released off the polysomes, and 3,557 mRNAs as unchanged during egg activation (Figures 1C and S2E; Table S4).

The discovery of a large number of translationally regulated mRNAs prompted us to employ an alternative genome-wide method to analyze the change in translational status of mRNAs at egg activation. Ribosome footprint profiling measures the number of ribosome-protected fragments (RPFs) derived from the mRNAs of each gene, which when normalized to mRNA abundance results in a single value for the translation efficiency (TE) of each gene (Ingolia et al., 2009). Moreover, ribosome

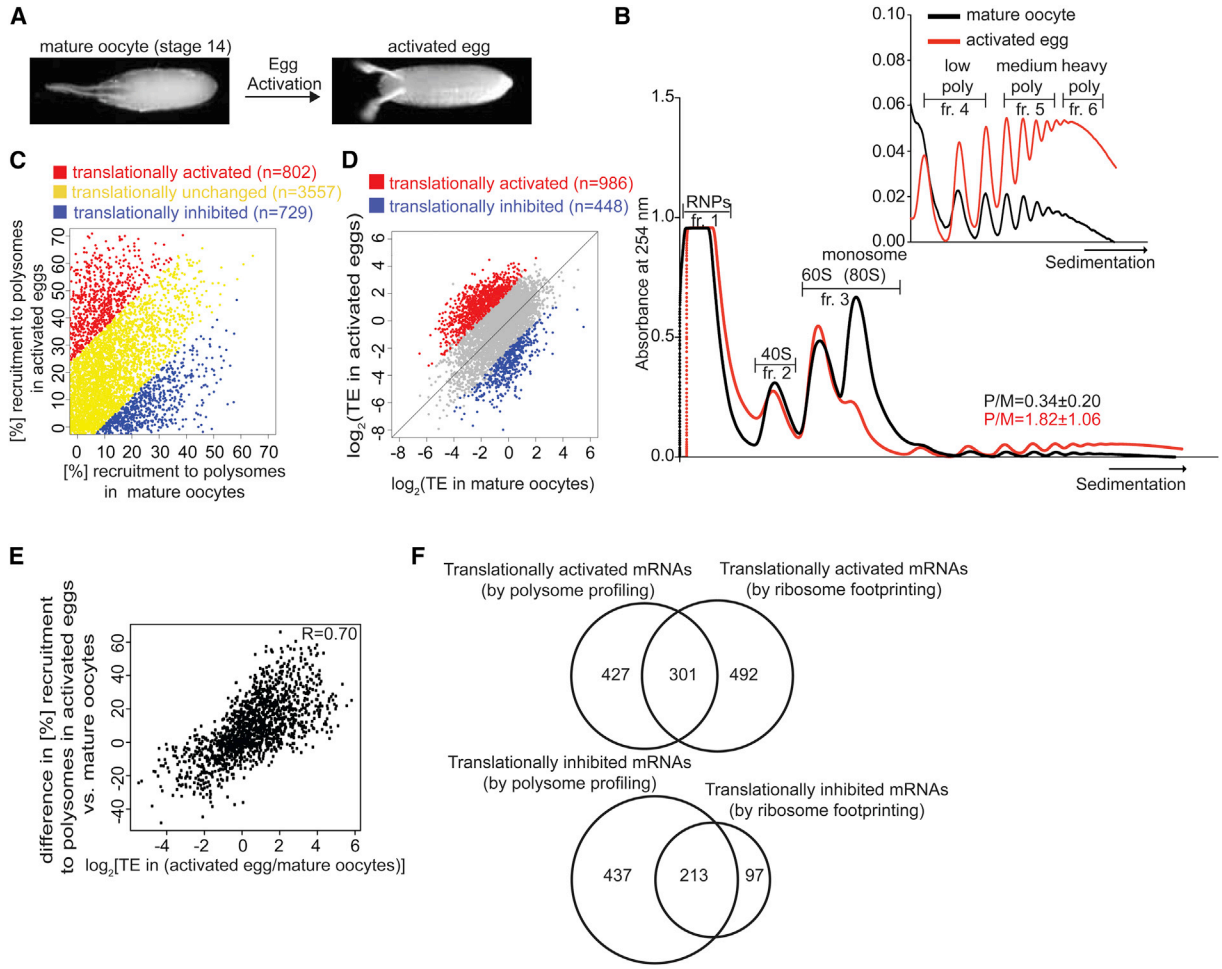

Figure 1. Translational Changes at Egg Activation

(A) Micrograph of a mature, stage 14 oocyte (preactivation state) and an activated egg (postactivation state). Anterior is on the left and dorsal is up.

(B) Representative profile of 254 nm absorbance for wild-type mature oocytes (black) and wild-type activated eggs (red). The inset is an enlargement of the polysomal section of the profile (starting from disomes). The six gradient fractions that were sequenced are labeled. Low polysomes correspond to 2–4 ribosomes, medium polysomes correspond to 5–9 ribosomes, and heavy polysomes correspond to ≥10 ribosomes. Polysome/monosome (P/M) ratios averaged from three biological replicate experiments are represented as mean ± SD.

(C) Comparison of mRNAs associated with polysomes (≥ 5 ribosomes) in mature oocytes and activated eggs. Data were corrected for the presence of mRNAs in the same regions of the gradient after fractionation of puromycin-treated samples. mRNAs were categorized as translationally inhibited (blue) if they had at least 9.1% higher polysomal recruitment in mature oocytes than in activated eggs. Translationally activated (red) mRNAs had at least 26.4% higher polysomal recruitment in activated eggs than in mature oocytes. The cutoffs were chosen because they are 1 SD from the mean difference for all the identified mRNAs. The remaining, translationally unchanged, mRNAs are shown in yellow; 5,088 mRNAs are represented as the mean of two biological replicates.

(D) Translation efficiencies (TEs, where TE = rpkm of RPFs/rpkm for mRNA abundance) in mature oocytes and activated eggs for 5,842 mRNAs. A total of 986 translationally activated mRNAs (red) have ~4.1-fold higher TE in activated eggs than in mature oocytes in both replicates, whereas for 448 translationally inhibited mRNAs (blue) the TE ratio is ~4.1-fold lower in activated eggs than in mature oocytes in both replicates. The cut-off of a ~4.1-fold change in TEs was chosen because it represents 1 SD of the ratios of TEs between activated eggs and mature oocytes in the samples prepared in the absence of cycloheximide. The mean of two biological replicates is shown.

(E) Correspondence between the two complementary methods to measure the translational status of mRNAs in activated eggs versus mature oocytes; 4,580 mRNAs, detected by both approaches, are shown as the average of two biological replicates for both experiments. The Spearman R value is indicated.

(F) The upper Venn diagram compares the number of mRNAs identified by polysome profiling (left) or ribosome footprinting (right) as translationally upregulated at egg activation, applying the criteria described in Figures 1C and 1D, respectively. The lower Venn diagram presents translationally inhibited mRNAs. Here and for all of the other Venn diagrams, only factors identified by both approaches (or in all compared samples) are represented.

See also Figures S1 and S2, and Tables S1 and S2.

footprinting reports the position of ribosomes on mRNAs. We observed an unusual accumulation of ribosomes on start codons specifically in mature oocytes, even though no cycloheximide was used (Figure S2F). This feature, however, seems to be unrelated to translational regulation for two reasons: (1) even in mature oocytes, RPFs at the start codon comprised only a small

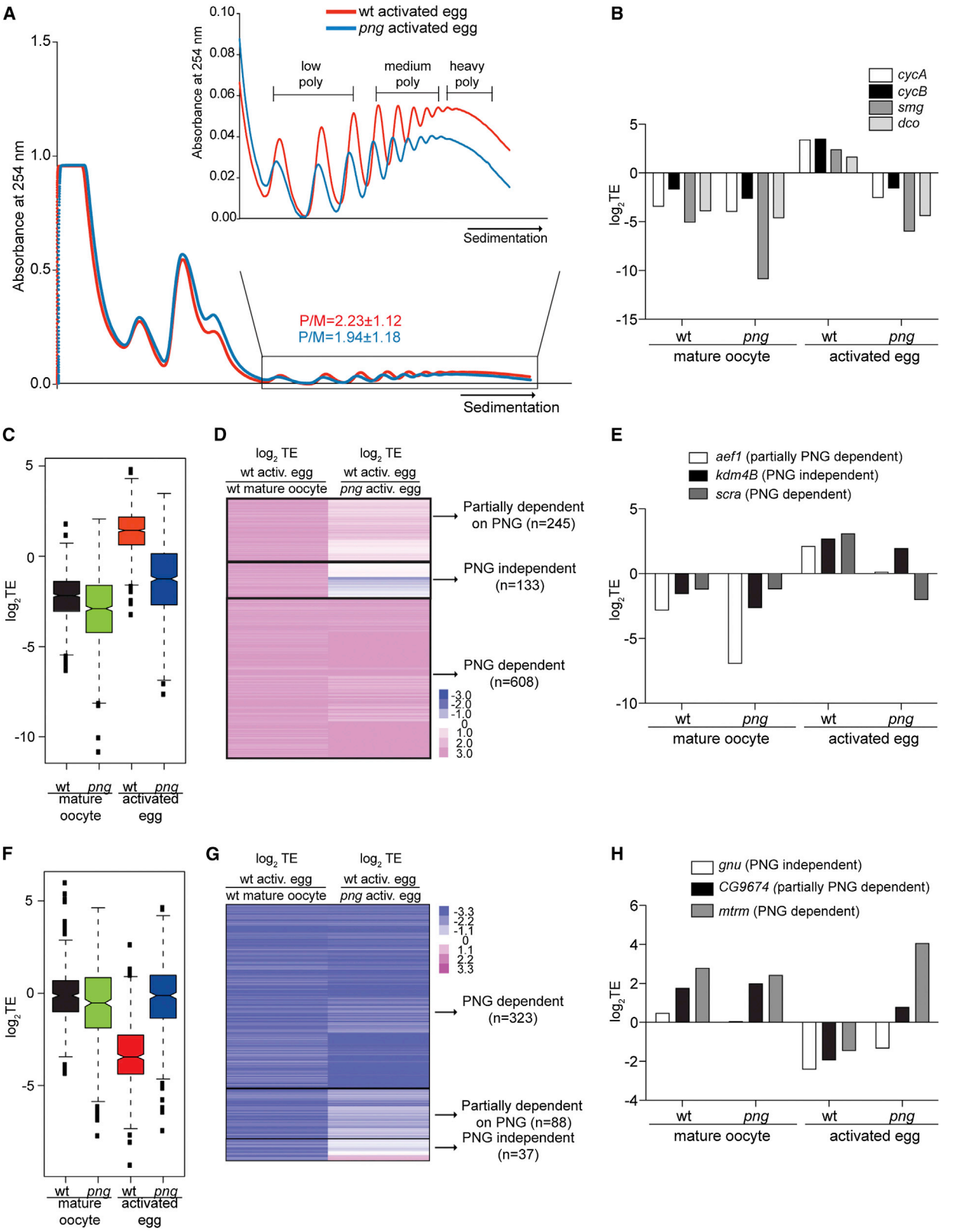

(legend on next page)

fraction of the RPFs for each gene (Figure S2F), and (2) initiation codon occupancy was not predictive of translational status in the activated egg (Figures S2G and S2H).

Two independent ribosome footprinting experiments yielded TE measurements for 5,842 mRNAs in mature oocytes and activated eggs (Figure S2I) and revealed drastic translational changes at egg activation (R = 0.37) (Figures 1D and S2J). *Mtrm*, the regulator of timing of oocyte maturation, and 447 other mRNAs were translationally repressed at egg activation, with ~4.1-fold lower TE in activated eggs than in mature oocytes. A total of 986 mRNAs, including positive controls such as the embryonic patterning mRNAs *bcd*, *hb*, *cad*, *tor*, *Tl*, and *smg*, as well as mRNAs encoding cell-cycle regulators (*cycA*, *cycB*, and *stg*), had ~4.1-fold higher TE in activated eggs than in mature oocytes and were translationally activated at egg activation (Tables S2 and S4). We found that 968 of the 986 mRNAs categorized as translationally activated at egg activation, and 390 of the 448 translationally repressed mRNAs were significantly translationally regulated with a p value of <0.05 between the two replicate experiments. If only a p value cutoff of < 0.05 is applied, 2,435 mRNAs would be considered translationally activated and 989 would be considered translationally repressed. Because the mRNAs identified as translationally regulated at egg activation using a ~4.1-fold-change cutoff were largely contained in the set selected by p value analysis, we chose the former approach for subsequent analyses, as it is more stringent.

The translational changes observed by ribosome footprinting and polysome profiling were in broad agreement (Spearman R = 0.70; Figure 1E), especially considering that these methods measure slightly different translational properties. Polysome profiling reveals the translationally active fraction of an mRNA. Ribosome footprinting provides information about the average number of ribosomes on each mRNA, with no insights as to whether only a small fraction of that mRNA is efficiently translated and the bulk is repressed.

Both methods identified 301 and 213 mRNAs as translationally upregulated or downregulated, respectively, at egg activation (Figure 1F). Our data set of 301 mRNAs translationally upregulated at egg activation was significantly enriched (false-discovery rate [FDR] < 0.05) for Gene Ontology (GO)-term categories such as "RNA processing," "mRNA binding," and "chromatin organization" (Figure S2K). Thus, translational activation might help prepare the egg for the maternal-to-zygotic transition, or these factors might serve transcription-independent roles during the first 2 hr of embryogenesis. Although hundreds of mRNAs were reported as translationally inhibited at egg activation in mice (Potireddy et al., 2006), none had been described in *Drosophila*. The 213 mRNAs we identified as translationally inhibited at egg activation showed enrichment in several GO-term categories, including "cell cycle process," consistent with egg activation involving completion of meiosis. Other enriched GO categories, such as "pyruvate metabolic process," "tRNA aminoacylation," and "nucleotide (ATP) binding," suggest that changes in metabolism or translation could be occurring at the exit of meiosis and entry into embryonic cycles (Figure S2L).

The PNG Kinase Is a Major Translational Regulator at Egg Activation

Having identified hundreds of mRNAs as translationally regulated at egg activation, our next goal was to discover key regulatory factors. One candidate was PNG, a Ser/Thr kinase that was previously demonstrated to promote translation of *cycB* and *smg* at egg activation (Tadros et al., 2007; Vardy and Orr-Weaver, 2007).

A slightly lower polysome/monosome ratio (P/M) in the *png* than wild-type activated eggs suggested a more systemic translational activation failure in *png* eggs (Figure 2A). These differences between wild-type and *png* activated eggs could not be attributed to mRNA expression levels, as mRNA abundance was highly correlated between these two samples (Pearson R = 0.99; Figure S3A). To identify translational targets of PNG, we performed ribosome footprinting of *png* mutant mature oocytes and activated eggs. The TEs of the positive controls, *cycB*, *cycA*, and *smg* were lower in *png* activated eggs than in wild-type (Figure 2B; Table S2). In *png* eggs, the TEs of all 986 mRNAs normally translationally upregulated at egg activation were closer to those of either wild-type or *png* mature oocytes than to those of wild-type activated eggs (Figure 2C).

A heatmap depicting the differences in TE in *png* activated eggs compared with the wild-type for each of the 986 translationally upregulated mRNAs shows that many, but not all, mRNAs require PNG function for activation (Figure 2D). A total of 608 mRNAs were dependent on PNG for their translational activation (e.g., *scra*; Figure 2E; Tables S2 and S4). In contrast,

Figure 2. PNG Kinase Regulates the Translational Status of the Majority of mRNAs at Egg Activation

(A) Representative profile of 254 nm absorbance for wild-type (WT, red) and *png* activated eggs (blue) as in Figure 1B, except that the P/M ratios are from two independent experiments.

(B) Graph showing the TEs of four mRNAs translationally upregulated at egg activation in WT, but not in *png* mutants (*png*).

(C) Box plot showing TEs in WT mature oocytes (black), *png* mature oocytes (green), WT (red), and *png* activated eggs (blue) for 986 mRNAs translationally upregulated at WT egg activation. The black lines within each box indicate the median, the edges of the boxes show the first and third quartiles of the values, and whiskers extend to the minimum and maximum values.

(D) A heatmap for 986 translationally activated mRNAs compares the TE ratios of WT activated eggs versus mature oocytes with the ratios of WT versus *png* activated eggs. Three classes defining dependence on PNG for translational activation at egg activation emerged. n, number of mRNAs in each category; TE, mean of two biological replicates.

(E) TEs in WT and *png* mature oocytes, as well as activated eggs, of three mRNAs representative of the three groups described in (D).

(F and G) Same as in (C) and (D), except that 448 translationally inhibited mRNAs are shown.

(H) Same as in (E), except that three mRNAs representative of the three groups classifying dependence on PNG for translational repression at egg activation are shown.

See also Figure S3 and Table S2.

we identified 133 mRNAs as PNG independent (e.g., *kdm4B*) and 245 as partially PNG dependent (e.g., *aef-1*; Figures 2D and 2E). We found that 38% of translationally activated mRNAs were at least partially independent of PNG, suggesting that there are one or more pathways acting in parallel to PNG to govern translation at egg activation, possibly serving divergent goals (Table S4). The PNG-independent pathway(s) may control translational activation of mRNAs encoding proteins involved in chromatin modifications (Figure S3B), whereas the PNG-dependent pathway seems to regulate mRNAs encoding protein kinases and factors involved in cell or tissue morphogenesis as well as embryonic development (Figure S3C).

We also found that many mRNAs translationally repressed at egg activation were dependent on PNG (Figure 2F). Based on differences in TEs in *png* versus wild-type activated eggs, we classified 323 mRNAs translationally inhibited at egg activation as dependent on PNG (e.g., *mtrm*), 37 as PNG independent (e.g., *gnu*), and 88 as partially PNG dependent (e.g., *CG9674*; Figures 2G and 2H; Tables S2 and S4). PNG-independent mRNAs were not enriched in any particular GO-term category (FDR > 0.05).

To examine the developmental timing when PNG is active, we tested whether PNG impacts the translational status of its target mRNAs prior to egg activation. The difference in TE for both translationally activated and repressed mRNAs was more pronounced between wild-type and *png* activated eggs than between mutant and wild-type mature oocytes ($p < 0.0001$; Figures 2C and 2F). Combining polysome profiling and quantitative RT-PCR (qRT-PCR), we found a similar distribution of four different candidate mRNAs within the sucrose gradients of wild-type and *png* mature oocytes (Figure S3D). These results indicate that mRNAs are translationally regulated by PNG at, but not prior, to egg activation.

Translational Upregulation Can Strongly Contribute to Increased Protein Levels at Egg Activation

Translational activity is well correlated with protein levels in *S. cerevisiae* growing in nutrient-rich media (Ingolia et al., 2009). However, the extent of coupling between the translatome and proteome has not been investigated in a developmental context. To assess proteome changes accompanying *Drosophila* egg activation, we compared unfertilized eggs with mature oocytes using a quantitative proteomics approach. Between 3,648 and 4,187 proteins were quantified in three biological replicate experiments (Figure S4A). At egg activation, comparing the change in protein levels with either a change in polysomal recruitment (Figures S4B and S4C) or a change in TE (Figures 3A and S4D) of the encoding mRNAs revealed a relatively poor correlation (R = 0.17 or 0.2, respectively). There were many examples of robust changes in TE corresponding to undetectable changes in protein levels. The correlation was not improved by considering changes in RPFs instead of changes in TE (Figure S4E). This is a consequence of egg activation occurring in the presence of constant mRNA levels (Figure S1A), thus resulting in a high correlation between changes in TE and changes in RPF (Spearman R = 0.99; Figure S4F).

We found that 291 proteins significantly increased after egg activation (FDR < 0.05; Figures 3A and 3B; Table S4). Among them were well-characterized regulators of early embryogenesis that served as our positive controls, such as the Cdc25 phosphatase String (Stg), as well as the embryonic patterning factors Toll and SMG (Edgar et al., 1994; Sallés et al., 1994; Tadros et al., 2007; Tables S3 and S4). The list of proteins that increased at egg activation was enriched in some of the same GO-term categories as mRNAs translationally activated at egg activation, i.e., chromatin organization and modification, as well as protein amino acid phosphorylation (Figure 3C). Additionally, the proteins upregulated at egg activation participated in a variety of other processes, supporting the complexity of this developmental transition (Table S4).

Approximately 40% of proteins whose levels increased at egg activation were encoded by mRNAs with a significant increase (>4.1-fold) in TE (category I, 89 proteins; Figure 3D; Table S4). Increased levels of several category I proteins were confirmed by immunoblots (Figures 3E and S4G). Overall, translational upregulation strongly contributed to increases in protein levels at egg activation, as the $\log_2$ median fold-change in TE for mRNAs encoding these proteins was 1.32 as compared with 0.14 for the entire quantified proteome. However, mechanisms other than translational regulation also play a role. For example, category II contains mRNAs that are not significantly translationally upregulated yet encode proteins whose levels are increased (Figures 3D and S4H; Table S4). In these cases, protein accumulation might be caused by posttranslational or other changes that stabilize these proteins and increase their half-life even in the absence of new synthesis. Alternatively, these proteins might be inherently more stable.

Surprisingly, only 25% of mRNAs identified as translationally activated by ribosome footprinting (or 20% in the case of polysome profiling) encoded proteins whose levels increased at egg activation (Figures 3A, 3D, S4B–S4D, and S4H; Table S4). The rest of the translationally activated mRNAs, category III, encoded proteins that were either unchanged (e.g., Dlg1; Figure 3E) or actually decreased (e.g., Dup; Figure S4G). For example, the level of Dlg1 remained unchanged at egg activation despite a 23.6-fold increase in the TE of its mRNA (Figure 3E). The level of Dup decreased 1.4-fold at egg activation, although the TE of its mRNA increased 2.6-fold (Figure S4G; Tables S2 and S3).

One possible explanation for the existence of category III (unchanged) proteins is that increased protein degradation offsets higher synthesis rates in activated eggs. An alternative explanation is that preexisting stores of these proteins greatly exceed the newly synthesized protein, such that increases from translation make up an undetectably small fraction of the total protein pool. We note that if preexisting protein stores generally obscured our ability to observe newly synthesized protein, this effect was independent of the starting amounts of protein, as we observed no significant difference in the abundance of category III compared with category I proteins in mature oocytes (two-sample Wilcoxon test, p = 0.09; Figures S4I–S4K). We also did not detect a significant difference in mRNA abundance between these two categories (two-sample Wilcoxon test, p = 0.17; Figure S4L).

Regardless of the mechanism involved, the imperfect relationship between changes in protein levels and changes in TE

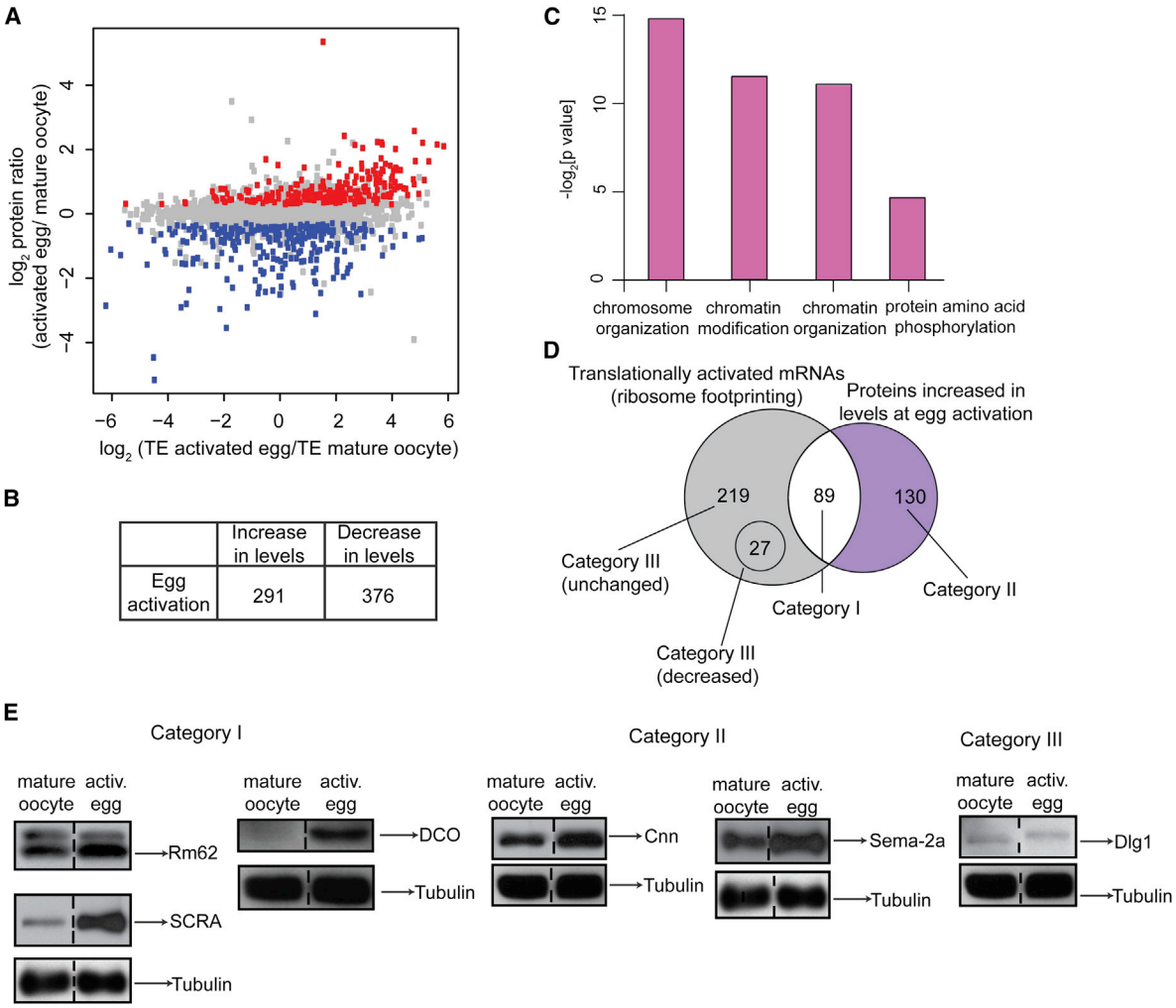

Figure 3. Protein Remodeling during the Oocyte-to-Embryo Transition

(A) Changes in protein levels and TE at egg activation. A scatterplot of the ratio of protein levels in activated eggs versus mature oocytes (mean of three biological replicates) and TE (mean of two biological replicates) is shown. The proteins that were scored as upregulated are shown in red and those scored as downregulated are in blue; 2,934 data points are presented (identified by both quantitative MS and ribosome footprinting).

(B) Table summarizing the number of proteins that had increased or decreased levels during egg activation.

(C) GO-term categories (FDR, $p < 0.05$) for proteins that were more abundant in activated eggs than in mature oocytes.

(D) Venn diagram comparing the number of translationally activated mRNAs (Figure 1D) that encode proteins upregulated at egg activation (category I). Proteins whose levels increased at egg activation according to quantitative MS without a corresponding increase in TE are shown in category II (violet). mRNAs identified by ribosome footprinting as being translationally upregulated at egg activation but encoding proteins with unchanged or decreased levels at egg activation are in category III (gray). Only factors identified by both approaches are represented.

(E) Western blot validation of candidates belonging to the categories described in (D). Rm62, SCRA (the same membrane reprobed), and DCO are validation examples for category I; Cnn and Sema-2a (reprobed on Rm62/SCRA membrane) are representative of category II; and Dlg1 (reprobed on Cnn membrane) is representative of category III. In this and all subsequent western blots, tubulin was used as a loading control. The dashed line marks that one lane from the original blot is not shown.

See also Figure S4 and Tables S3 and S4.

highlights the value of our integrated approach. When we considered translational changes that were most relevant for egg activation, the acquisition of quantitative proteomics data enabled us to focus on those that had the greatest impact on protein levels (category I). Moreover, proteomics measurements revealed some changes that were not detectable when we examined translation changes (category II), whereas translation measurements uncovered translationally activated mRNAs that were not detectable when we examined only protein changes (category III).

Lid Activity Is Required in Early Embryogenesis

The limited number of proteins that increase at activation may represent factors that are critical for early embryonic development. It was interesting that the levels of three histone demethylases significantly increased at egg activation, given that early

embryonic development in *Drosophila* is transcriptionally silent. The levels of Little Imaginal Discs (Lid) were increased 2.7-fold at egg activation, whereas those of Kdm4A and Kdm4B increased 3.6- and 2.3-fold, respectively (Table S3). Lid is a conserved and essential histone H4-me3-specific demethylase that has been shown to regulate gene expression, particularly of *hox* genes (Gildea et al., 2000; Lloret-Llinares et al., 2008), but it also may be involved in growth control through its association with dMyc (Secombe et al., 2007).

To study the role of Lid in the oocyte-to-embryo transition, we depleted Lid in the female germline by expressing RNAi against *lid* using the UAS-GAL4 system. qRT-PCR analysis of *lid* levels in mature oocytes of two different *lid* RNAi-expressing lines revealed that they were about 99% lower than in the control, demonstrating efficient knockdown (Figure S5A). Importantly, meiotic progression was not perturbed upon *lid* knockdown, as evidenced by metaphase I plate morphology that was comparable to that of the control (Figures S5B and S5C).

To examine the consequence of *lid* ablation on the early embryonic mitotic divisions, we measured the progression through early embryonic cycles by counting the percentage of laid embryos that (1) completed meiosis and thus contained polar bodies arranged into rosettes, but did not initiate embryonic divisions; (2) completed one to four embryonic cycles; (3) completed five to nine embryonic cycles; or (4) reached the syncytial blastoderm, corresponding to division cycles 10–13 (Figures 4A and S5D). The embryos from *lid* RNAi-ablated mothers showed slower progression through embryogenesis than the control. In particular, increased numbers of embryos were in the rosette stage or going through the first-to- fourth embryonic cycles. Consequently, fewer embryos reached later cycles (Figure 4A). There were subsequent embryonic defects, including a reduction in the number of gastrulating embryos and the appearance of embryos with pycnotic or aberrantly aggregated nuclei (Figures 4B and 4C). These data indicate that Lid has a role unrelated to transcription that is required during early embryogenesis for proper further embryonic development.

PNG-Mediated Translational Upregulation Provides Insights into the Balance of Translation and Protein Degradation for a Subset of Proteins

It was striking that at egg activation the majority of translationally activated mRNAs encoded proteins whose levels remained equal or even decreased (Figures 3D and S4B–S4D). To test the importance of translational upregulation for those mRNAs, we compared the proteomes of wild-type activated eggs with eggs laid by mothers mutant for the translational regulator PNG (Figure S6A; Table S3). The majority of proteins that increased at egg activation and were encoded by translationally upregulated mRNAs had lower levels in *png* eggs than in wild-type eggs (46 out of 75; Table S4; Figure 5A). Consistently, ~80% of these 46 mRNAs completely depended on PNG for translational upregulation at egg activation (Figure 5B). The other 29 mRNAs encoded proteins with unchanged levels in *png* activated eggs as compared with wild-type (Figures 5A and S6B; Table S4), most likely because a large fraction of them (~59%) were at least partially independent of PNG for their translational activation at egg activation (Figure 5B).

Interestingly, there were 63 translationally upregulated mRNAs that encoded proteins with stable levels at egg activation but decreased abundance in *png* as compared with wild-type activated eggs (orange segment in Figures 5A and S6B; Table S4). We found that 86% of these 63 mRNAs were dependent on PNG for their translational upregulation at egg activation (Figure 5B). This group of proteins, represented by Dlg1, suggested that translational upregulation at egg activation might even be influencing proteins whose abundance does not change (Figure 5C). Another possibility was that inefficient maternal protein deposition in *png* mature oocytes led to the lower levels of proteins in *png* activated eggs versus wild-type (orange segment of Figure 5A), although this was not the case for Dlg1 (Figure 5C). In addition, the majority of these 63 proteins were present at lower levels in *png* activated eggs as compared with *png* mature oocytes (Figures S6B and S6C; Table S3). Collectively, these results are consistent with the possibility that, for a subset of proteins, translational upregulation compensates for protein turnover occurring at egg activation to maintain rather than increase their levels at this developmental transition.

Downregulation of Protein Levels at Egg Activation Is Largely Posttranslationally Driven

A quantitative comparison of the proteomes of mature oocytes and activated eggs revealed that 376 proteins became significantly less abundant at egg activation ($p < 0.05$; Figures 3A and 3B; Table S4). This group was not enriched in any particular GO category (FDR > 0.05). Downregulation of proteins can be at least partially attributed to the activation of the APC/C at the completion of meiosis, resulting in the proteasomal degradation of its substrates, such as cell-cycle regulators CycB3 and Mtrm (Pesin and Orr-Weaver, 2007; Whitfield et al., 2013). In addition, other degradation pathways are likely to be active.

For 265 of 376 significantly downregulated proteins, we obtained TE information about their mRNAs and found that 43 were translationally downregulated (category IV; Figure 6A; Table S4). In agreement with the proteomics data, immunoblots showed that the levels of Giant Nuclei (GNU, category IV) decreased after egg activation (Figure 6B). The number of downregulated proteins encoded by translationally inhibited mRNAs is significant, as only six of the translationally repressed mRNAs encode proteins whose levels increased during egg activation ($p < 10^{-7}$; Figure 6A). The levels of 226 proteins encoded by translationally inhibited mRNAs were not decreased at egg activation, presumably because the maternal stockpiles of these proteins are stable. We obtained comparable results when we measured the translation status at egg activation as a change in polysomal recruitment (Figure S6D).

Category V proteins showed decreased levels at egg activation even though their encoding mRNAs retained their translational status (Table S4). For example, CycB3 protein was reduced 5.6-fold although the TE of its encoding mRNA increased 7.6-fold (Tables S2 and S3). Most of the proteins that were downregulated at egg activation have not been studied for their role in meiosis, and many are completely

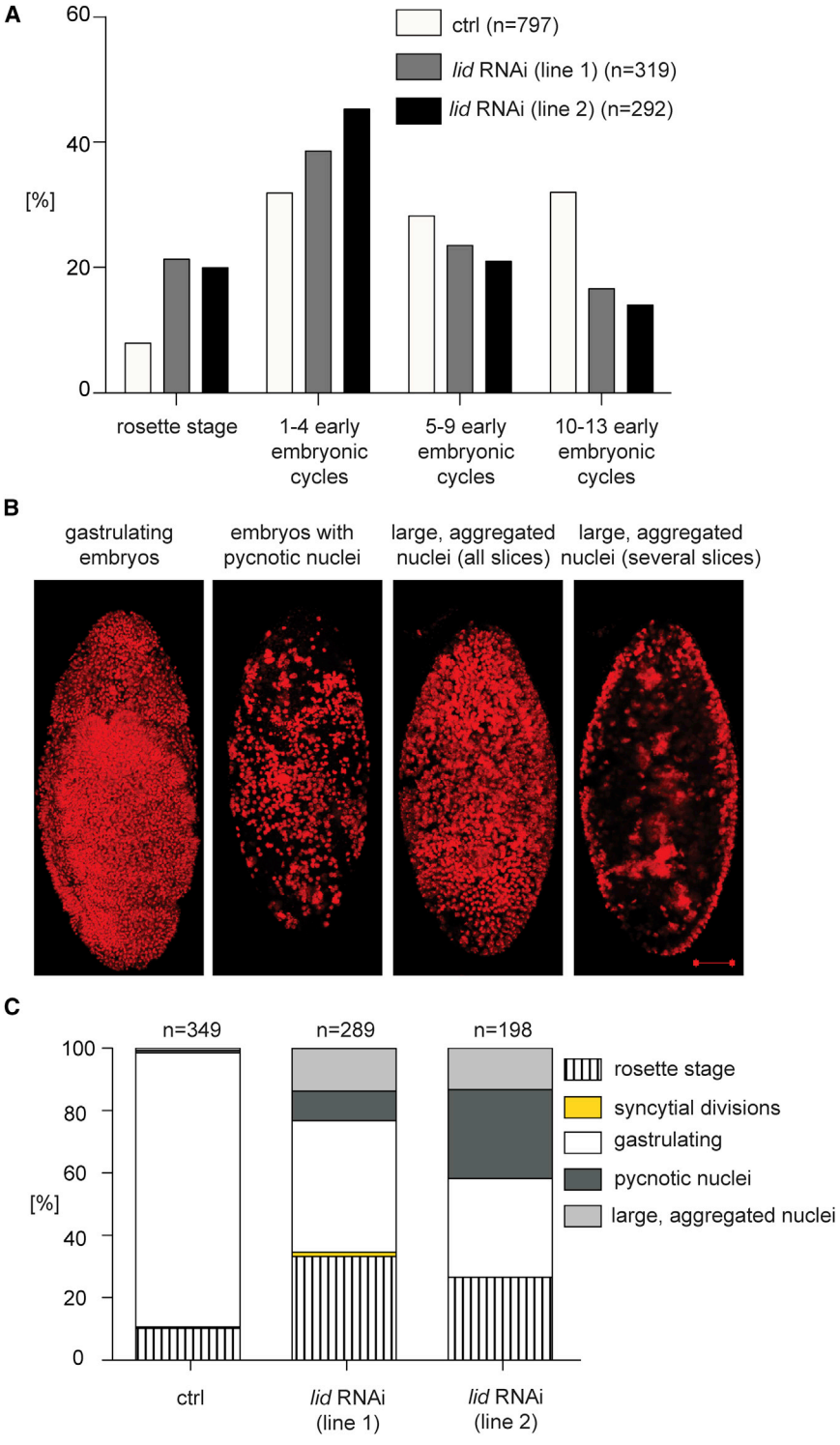

Figure 4. The Histone H3K4 Demethylase *lid* Is Required for Proper Early Embryonic Development

(A) Quantification of the percentage of 0–2 hr embryos that were present in different cycles of embryogenesis after completion of meiosis (as shown in Figure S5D). Embryos were laid either by mothers with only the *maternal* α-*tubulin-Gal4* driver (control) or by mothers in which a *lid* RNAi line was expressed using the *mat*α-*tubulin-Gal4* driver. *lid* RNAi line 1 is BL35706; line 2 is BL36652. One representative experiment is shown. n, number of embryos scored.

(B) Representative images of 0–2 hr embryos that were aged for an additional 3 hr and stained with a DNA stain (propidium iodide, red). For gastrulating embryos (control) and embryos with pycnotic or aggregated nuclei laid by mothers expressing *lid* RNAi, maximal intensity projections of z stacks are shown. For embryos with large, aggregated nuclei, the figure shows the maximal intensity projections of the entire embryo as well as the optical sections in which aggregated nuclei are particularly visible. In all panels, the dorsal side of the embryo is shown with anterior at the top. Scale bar, 50 μm.

(C) Percentage of properly developed (gastrulating) and aberrantly developed embryos that were collected for 2 hr and aged for an additional 3 hr. Aberrantly developed embryos were classified as still at the rosette stage, in syncytial divisions, gastrulating, or displaying pycnotic or aggregated nuclei (as shown in B). The same genotypes as in (A) were examined. n, number of embryos scored. See also Figure S4.

uncharacterized. In addition to revealing candidate regulators of the oocyte-to-embryo transition, these results indicate that for most of the proteins that were downregulated at egg activation, posttranslational rather than translational control governed the decrease in protein levels at egg activation. Most of these downregulated proteins decreased without translational inhibition of their mRNAs.

Failure in Translational Inhibition for a Subset of mRNAs Interferes with Successful Removal of the Proteins They Encode at the Oocyte-to-Embryo Transition

The modest contribution of translational inhibition to decreased protein levels at egg activation suggested that many of the proteins that were reduced at egg activation in the wild-type would also be reduced in the *png* mutant background. Indeed, 289 proteins were significantly reduced in *png* activated eggs as compared with *png* mature oocytes, and 193 of them were among the 283 proteins that were significantly reduced in wild-type eggs at activation (Figure 6C). Nonetheless, 42 proteins that were reduced at egg activation in the wild-type had higher levels in *png* versus wild-type activated eggs (Figure 6D). Approximately 31% of these proteins, including Mtrm, were encoded by mRNAs that were dependent on PNG for their translational shutoff. Consequently,

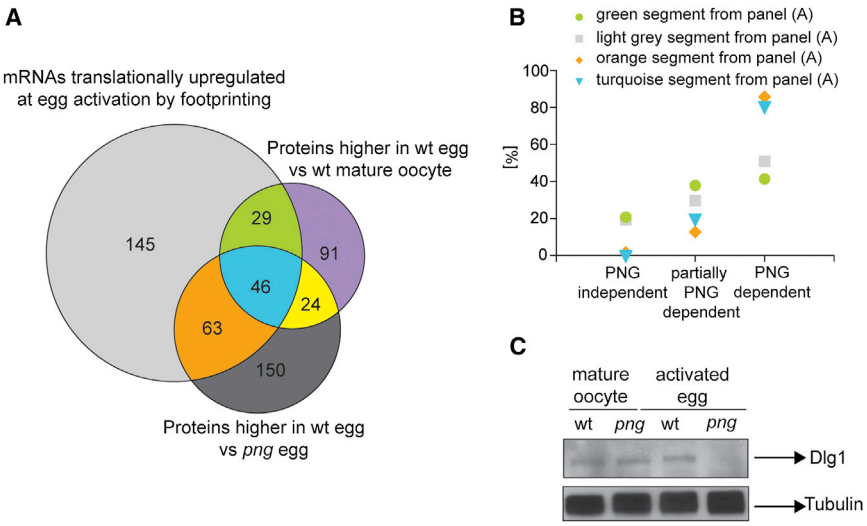

Figure 5. The Translational Regulator PNG Reveals the Importance of Translational Regulation for Homeostasis of Protein Levels for a Subset of Proteins at Egg Activation

(A) Same as Figure 3D, except that the comparison included the proteins whose levels are higher in WT than *png* activated eggs according to MS. Only factors identified in all compared samples are represented. The translationally upregulated mRNAs are from the WT.

(B) Percentage of mRNAs encoding proteins belonging to the light gray, orange, green, or turquoise segments in (A) that are independent, partially dependent, or dependent on PNG for translational upregulation at egg activation.

(C) Western blot validation of Dlg1, a candidate from the orange segment of the Venn diagram in (A). Dlg1 levels do not change at egg activation in the WT, although the protein shows altered mobility. In contrast, protein levels are decreased following activation of *png* mutants (reprobed on the same membrane as in Figure 6F).

See also Figure S6 and Tables S3 and S4.

their TEs were overall significantly higher in *png* than in wild-type eggs (Mann-Whitney test, $p < 0.0001$; Figure 6E; Table S4).

The absence of a translational shutoff in *png* eggs allowed us to investigate the role of translational inhibition in decreased protein levels at egg activation, using Mtrm as an example. In parallel, we employed the *mr* mutant, which carries a mutation in the APC2 subunit, to weigh the contributions of APC/C-mediated proteasomal degradation versus translational inhibition to Mtrm protein levels (Kashevsky et al., 2002). Western blotting confirmed the proteome data showing that although there was a substantial decrease in Mtrm levels in both wild-type and *png* activated eggs as compared with mature oocytes, there was persistent Mtrm protein in *png* eggs (Figure 6F). Because the Mtrm levels that remained in *png* activated eggs were lower than those in *mr* activated eggs, we conclude that Mtrm levels are primarily regulated by targeting via the APC/C for proteasomal degradation. Thus, optimal protein decrease at egg activation in addition to protein degradation may require a PNG-dependent shutoff of translation.

DISCUSSION

Relationship between the Translatome and the Proteome

This study provides a demarcation of the contribution of translational and posttranslational regulation to proteome remodeling during a key developmental transition from oocyte to embryo. This transition requires a change from meiosis to mitosis as well as resetting of the oocyte to restore totipotency in the embryo. The absence of transcription and mRNA degradation in the oocyte and early embryo leads to exclusively translational and posttranslational control of gene expression. In this study, the oocyte-to-embryo transition was assessed through quantitative proteomics analysis combined with complementary translatome measurements. We found that translational upregulation strongly contributes to increased protein levels at egg activation. The effect of translational shutdown on decreased protein levels is more modest, with decreased levels appearing to be largely driven by protein degradation.

The striking translational changes that occurred at egg activation, with as many as 802–986 translationally upregulated and 448–729 inhibited mRNAs, are comparable to those observed in other developmental studies. Polysome profiling at oocyte maturation and egg activation in mouse or in different stages of *Drosophila* embryogenesis also showed that hundreds of mRNAs were both released from and recruited to the polysomes (Chen et al., 2011, 2014; Potireddy et al., 2006; Qin et al., 2007). Thus, this window of development is highly dynamic across species and it relies on translational control.

Mechanism of Translational Control at Egg Activation

We observed both activation and inhibition of mRNA translation at the oocyte-to-embryo transition. Translational inhibition at egg activation may not be an actively regulated process. Rather, the onset of increased translational activity observed at egg activation may limit the available ribosomes, resulting in reduced access to ribosomes and consequently translational repression for the subset of mRNAs.

The Ser/Thr kinase PNG was previously demonstrated to activate the translation of *cycA*, *cycB*, and *smg*, but given the specificity of the mutant phenotypes and results from rescue experiments with overexpression of *cycB*, it was assumed to influence a circumscribed set of targets (Lee et al., 2001). In contrast, we find that PNG is a global regulator of the translational status of mRNAs exclusively at egg activation. In addition, although PNG has been thought to activate translation, our analysis reveals that it acts both positively and negatively, controlling the translational activation of at least 60% of regulated mRNAs and inhibition of 70%. Despite the critical role of PNG in controlling the translational status of the majority of mRNAs at egg activation, it is unlikely that the primary function of PNG kinase is to mediate an activation event upstream in the

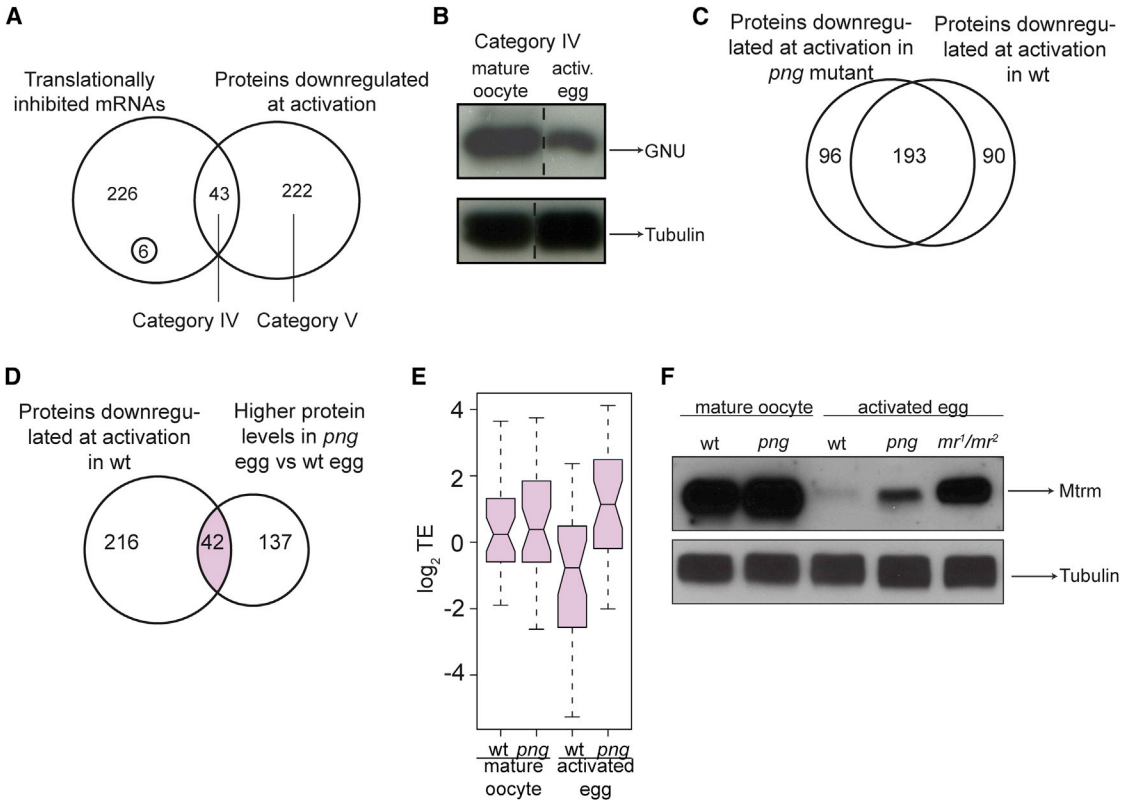

Figure 6. The Absence of a Translational Shutdown at Egg Activation May Interfere with Efficient Downregulation of a Subset of Proteins

(A) Venn diagram showing the number of translationally inhibited mRNAs (Figure 1D) that encode proteins downregulated at egg activation (category IV). Other proteins whose levels decrease at egg activation according to quantitative MS are in category V. Among translationally inhibited mRNAs there are two groups: the majority of mRNAs encode proteins with unchanged levels at egg activation, whereas only six encode proteins whose levels increase. Only factors identified in both samples are represented.

(B) Western blot validation of GNU, a protein from category IV.

(C and D) Venn diagrams comparing the number of proteins that according to MS are downregulated at egg activation in WT or *png* activated eggs (C) or downregulated at activation in WT but more abundant in *png* activated eggs than in WT (D). Only factors identified in both compared samples are represented.

(E) Box plot showing TEs of mRNAs encoding for 36 proteins in the overlap zone (shown in light pink) of Venn diagram in (D). Only 36 out of 42 mRNAs are presented because the other six were not identified by ribosome footprinting.

(F) Western blot comparing Mtrm levels at egg activation in WT and *png* mutant background as well as in the activated eggs laid by mothers transheterozygous for female-sterile alleles of the APC2 subunit of APC/C, *morula* (mr^1/mr^2). In *png* mutants in which translational inhibition of *mtrm* does not occur, Mtrm protein levels are elevated, although to a lesser extent than when the APC/C is mutated.

See also Figure S6 and Tables S3 and S4.

egg activation pathway. Many activation events, such as eggshell hardening (Tadros et al., 2003) and downregulation of protein levels, occur in *png* mutants.

We postulate that many of the PNG-dependent translational effects reflect a direct role of the kinase. It will be interesting to investigate PNG substrates for candidates whose phosphorylation affects the TEs of mRNAs. It is likely, however, that translation of some mRNAs may be affected as a secondary or indirect effect of PNG activity.

One possible direct target of PNG that affects translation is the translational repressor Pumilio (PUM). The *png* embryonic cell-cycle defect is suppressed by *pum* mutations, which restore Cyclin B protein levels (Vardy and Orr-Weaver, 2007). PNG-PUM antagonism does not appear to be an exclusive mechanism through which PNG mediates translational activation, as there is no enrichment of PUM-binding sites in the 3′ UTRs of PNG-dependent translationally activated mRNAs compared with PNG-independent mRNAs (see Supplemental Discussion for additional 5′ and 3′ UTR analyses). This suggests that PNG controls translation via multiple targets. Some of its targets may also be translational regulators, as CG17514, a putative activator of translation, is translationally downregulated, whereas the translational repressor Cup is translationally upregulated, in *png* activated eggs.

The large number of puromycin-insensitive mRNAs we observed in mature oocytes was surprising and suggests that many mRNAs are localized to cytoplasmic granules or heavy RNPs at this developmental stage. The inefficient translation of these mRNAs in mature oocytes was corroborated by ribosome footprinting analysis, as they were found to associate with significantly fewer ribosomes compared with puromycin-sensitive

mRNAs (data not shown). Since puromycin only displaces actively translocating ribosomes, a fraction of puromycin-insensitive mRNAs may localize to cytosolic compartments where they are associated with stalled and nonelongating polysomes.

There is precedent for the notion that specific mRNAs are localized to cytoplasmic granules in oocytes. In *Drosophila*, the maternally deposited mRNAs for three patterning genes, *osk*, *grk*, and *bcd*, localize to large RNP complexes (Chekulaeva et al., 2006; Weil et al., 2012). It has been suggested that these cytoplasmic RNPs control both activation and repression of translation: *grk* mRNA is on the periphery of the complex and translated, whereas the internally localized *bcd* mRNA is repressed (Weil et al., 2012). Cytosolic granule association also may serve as a timer for translational activation. In zebrafish and mouse oocytes, association of *cycB* mRNA with cytosolic granules is not necessary for translational repression, but release out of the granules leads to premature CycB synthesis (Kotani et al., 2013).

Insights into Key Regulators of the Oocyte-to-Embryo Transition

By identifying translationally regulated mRNAs and proteins whose levels change at egg activation, this work also highlights potential key processes in the oocyte-to-embryo transition and reveals previously unrecognized regulators. As a proof of principle, we demonstrated that one of the 291 proteins that are upregulated at egg activation, the histone H3K4 demethylase LID, is required for timely progression through early embryonic cycles and proper further embryonic development. Other upregulated proteins may be required immediately at the onset of embryogenesis.

Downregulation of specific proteins at the oocyte-to-embryo transition also is important. This has been demonstrated for the Polo kinase inhibitor Mtrm, whose degradation is required for proper embryogenesis (Whitfield et al., 2013). The microtubule-severing enzyme katanin subunit Kat80 is controlled similarly (Tables S1–S4). In *C. elegans*, katanin (MEI-1) is required for assembly of the meiotic spindle, but failure to decrease its levels before embryonic mitosis leads to spindle defects (Quintin et al., 2003; Stitzel et al., 2006). The translational inhibition applied to these mRNAs may combine with proteasomal degradation for faster and more complete removal of meiotic proteins.

"Resetting" the Proteome at the Oocyte-to-Embryo Transition

Our translatome and proteome survey of *png* eggs provided an unexpected insight into the possible coupling of translational regulation and protein degradation at egg activation. There is a class of 63 mRNAs that are translationally upregulated without a perceptible increase in their protein levels in wild-type eggs. These proteins seem to be properly maternally deposited in *png* mutant oocytes, but their mRNAs require PNG for translational upregulation at egg activation. Lower levels of these proteins in *png* versus wild-type activated eggs showed that a failure of translational activation resulted in easily detected decreases in protein levels. Hence, the apparently constant levels of these proteins in the wild-type background were not merely a consequence of high maternal stores overwhelming the translational activation. Moreover, the proteome changes in *png* mutants are unlikely to result from an additional independent effect of PNG on protein stability, as quantitative mass spectrometry (MS) data show that downregulation of protein levels occurs comparably in wild-type and *png* mutants eggs.

Thus, the simplest explanation for these results is that translational activation compensates for protein degradation, leading to no net change in protein abundance in the wild-type background. Although the *png* mutant allowed us to demonstrate this for 63 proteins, it is likely that additional proteins are reset. An additional possibility is that for some of these proteins, there is a spatial control in the embryo, with synthesis at one site and degradation at another. The increased protein degradation that normally occurs at egg activation probably is supported by mechanisms in addition to the APC/C, as we found at least 11 E2 Ubiquitin-conjugating enzymes, E3 Ubiquitin ligases, or their putative regulators among the proteins that were upregulated at egg activation.

The conclusions from our analysis of developmental control of the proteome at *Drosophila* egg activation contrast with a previous study in mouse fibroblasts in which the contribution of protein degradation to protein abundance is minor (Schwanhäusser et al., 2011). Unlike *Drosophila* activated eggs, mouse fibroblasts are transcriptionally active, a steady-state system that lacks maternally loaded proteins, potentially resulting in different requirements for translational regulation in controlling protein levels.

Why would a subset of proteins in activated eggs undergo an energetically costly process of increased synthesis and degradation only to maintain the same levels as in mature oocytes? We suggest that the developmental coordination between translation and protein stability restores the proteome, changing these proteins from their "oogenesis" form to their "embryogenesis" form. As some posttranslational modifications might interfere with the embryonic functions of a given protein, an expedient mechanism to remove these modifications might be to degrade and then resynthesize the proteins. Such a "resetting" of this subset of the proteome at egg activation resembles a phenomenon that occurs later in embryogenesis at the midblastula stage, in which the transcriptome is reset to allow zygotic control of development (Tadros and Lipshitz, 2009).

EXPERIMENTAL PROCEDURES

Quantitative Mass Spectrometry

Mature oocytes were hand dissected in Grace's Unsupplemented Insect Media (Gibco) from 4-day-old flies that had been fattened for 3 days with wet yeast at 22°C. Activated eggs collected for 0–2 hr (laid by wild-type *Oregon R* females mated with spermless *twine* ^{HB5} males) were dechorionated, lysed, and sonicated, and the supernatants were frozen. Digestion of the proteins and stable isotope labeling of the peptides (peptide dimethylation) were performed as previously described (Wiśniewski et al., 2009; Boersema et al., 2009). The labeled peptides were fractionated, desalted, and separated using the nanoAcquity UPLC system (Waters), from which they were directed to an LTQ Orbitrap Velos (Thermo Fisher Scientific) using a Proxeon nanospray source. The MS raw data were processed using MaxQuant (version 1.1.1.25) (Cox and Mann, 2008) and MS/MS spectra were searched using the Andromeda search engine (Cox et al., 2011) against a Uniprot *Drosophila melanogaster* database. Statistical analysis of MS data was performed using the Limma package in R/Bioconductor (Gentleman et al., 2004). Further details are provided in Supplemental Experimental Procedures.

Western Blots

Samples were lysed and western blots performed as previously described (Whitfield et al., 2013). The antibodies used are described in Supplemental Experimental Procedures.

Polysome Analysis, Ribosome Footprint Profiling, RNA Isolation, and mRNA-Seq

Samples were lysed as described previously (Mermod and Crippa, 1978) and flash frozen. For puromycin treatment, samples were prepared as described previously (Clark et al., 2000). The samples were run on 10%–50% linear sucrose gradients with 0.5 mg/ml cycloheximide. Cycloheximide was excluded for the gradients in the puromycin-treatment experiments. Following centrifugation and fractionation, prior to RNA extraction, 5 ng of in vitro transcribed Firefly luciferase (5 ng; Promega) and 5 ng of *S. cerevisiae* mRNA were added to each pooled fraction to allow for normalization between the fractions.

RNA was isolated from whole lysates of mature oocytes or activated eggs by homogenizing them in TRIzol (Invitrogen) according to the manufacturer's instructions. To extract RNA from sucrose gradient fractions, 0.5% SDS and 200 μg/ml of Proteinase K (Sigma-Aldrich) were added for 30 min at 50°C, followed by RNA isolation using the hot acid phenol method.

For ribosome footprint profiling, samples were thawed on ice and then triturated four times with a 26-gauge needle. After centrifuging to clear the lysate, ribosome profiling and mRNA-seq were performed as described previously (Subtelny et al., 2014) using a detailed protocol available at http://bartellab.wi.mit.edu/protocols.html. A replicate of each sample was prepared with cycloheximide excluded from all solutions.

To sequence mRNAs, 1 μg of total RNA was poly(A) selected using SeraMag magnetic oligo(dT) magnetic particles (Thermo Scientific). Barcoded mRNA-seq libraries were made according to the manufacturer's instructions (Illumina), with the exception that mRNA was fragmented using a RNA fragmentation kit (Ambion). The mRNA-seq analysis is described in Supplemental Experimental Procedures.

The average TE from two independent ribosome footprinting experiments obtained by our method of isolating and preparing lysates from 0–2 hr unfertilized eggs correlated well (Spearman R = 0.89) with TEs recently published for fertilized 0–2 hr embryos cryolysed in the absence of dechorionation (Dunn et al., 2013).

Immunofluorescence and Imaging

Embryos were collected at 25°C for 2 hr (and, if indicated, aged for an additional 3 hr at 25°C), dechorionated, fixed, and stained as described previously (Pesin and Orr-Weaver, 2007). Images were acquired on an LSM 700 microscope (Carl Zeiss) and processed using ImageJ software.

ACCESSION NUMBERS

The polysome profiling and ribosome footprinting sequencing data reported in this work have been deposited in the Gene Expression Omnibus (www.ncbi.nlm.nih.gov/geo/) under accession number GSE52799.

SUPPLEMENTAL INFORMATION

Supplemental Information includes Supplemental Discussion, Supplemental Experimental Procedures, six figures, and four tables and can be found with this article online at http://dx.doi.org/10.1016/j.celrep.2014.05.002.

ACKNOWLEDGMENTS

We thank A. Amon, W. Gilbert, J. Richter, M. Hara, B. Petrova, O. Rissland, and I. Ulitsky for helpful comments on the manuscript. We are grateful to J. Kirkpatrick from the EMBL Proteomics Core Facility for help in processing the samples for quantitative MS analysis. We thank G. Bell for help with bioinformatics analysis and T. DiCesare for help with the graphical abstract. We acknowledge A. Imhof, J. Brill, J. Price, T. Kaufman, E. Wahle, and M. Asano for the kind gifts of antibodies. The Sema-2a and Dlg1 antibodies developed by C. Goodman were obtained from the Developmental Studies Hybridoma Bank. We thank the TRiP at Harvard Medical School (NIH/NIGMS R01-GM084947) and the Bloomington Stock Center for providing the transgenic RNAi fly stocks used in this study. I.K. was supported by a Feodor Lynen Postdoctoral Fellowship from the Alexander von Humboldt Foundation. This research was funded by NIH grant GM39341 (to T.L.O.-W.). D.P.B. is an HHMI investigator and T.L.O.-W. is an American Cancer Society Research Professor.

Received: November 4, 2013
Revised: March 10, 2014
Accepted: May 1, 2014
Published: May 29, 2014

REFERENCES

Anderson, K.V., and Lengyel, J.A. (1979). Rates of synthesis of major classes of RNA in Drosophila embryos. Dev. Biol. *70*, 217–231.

Beilharz, T.H., and Preiss, T. (2004). Translational profiling: the genome-wide measure of the nascent proteome. Brief. Funct. Genomics Proteomics *3*, 103–111.

Blobel, G., and Sabatini, D. (1971). Dissociation of mammalian polyribosomes into subunits by puromycin. Proc. Natl. Acad. Sci. USA *68*, 390–394.

Boersema, P.J., Raijmakers, R., Lemeer, S., Mohammed, S., and Heck, A.J. (2009). Multiplex peptide stable isotope dimethyl labeling for quantitative proteomics. Nat. Protoc. *4*, 484–494.

Brar, G.A., Yassour, M., Friedman, N., Regev, A., Ingolia, N.T., and Weissman, J.S. (2012). High-resolution view of the yeast meiotic program revealed by ribosome profiling. Science *335*, 552–557.

Carlile, T.M., and Amon, A. (2008). Meiosis I is established through division-specific translational control of a cyclin. Cell *133*, 280–291.

Charlesworth, A., Meijer, H.A., and de Moor, C.H. (2013). Specificity factors in cytoplasmic polyadenylation. Wiley Interdiscip. Rev. RNA *4*, 437–461.

Chekulaeva, M., Hentze, M.W., and Ephrussi, A. (2006). Bruno acts as a dual repressor of oskar translation, promoting mRNA oligomerization and formation of silencing particles. Cell *124*, 521–533.

Chen, J., Melton, C., Suh, N., Oh, J.S., Horner, K., Xie, F., Sette, C., Blelloch, R., and Conti, M. (2011). Genome-wide analysis of translation reveals a critical role for deleted in azoospermia-like (Dazl) at the oocyte-to-zygote transition. Genes Dev. *25*, 755–766.

Chen, L., Dumelie, J.G., Li, X., Cheng, M.H., Yang, Z., Laver, J.D., Siddiqui, N.U., Westwood, J.T., Morris, Q., Lipshitz, H.D., and Smibert, C.A. (2014). Global regulation of mRNA translation and stability in the early Drosophila embryo by the Smaug RNA-binding protein. Genome Biol. *15*, R4.

Chu, S., and Herskowitz, I. (1998). Gametogenesis in yeast is regulated by a transcriptional cascade dependent on Ndt80. Mol. Cell *1*, 685–696.

Clark, I.E., Wyckoff, D., and Gavis, E.R. (2000). Synthesis of the posterior determinant Nanos is spatially restricted by a novel cotranslational regulatory mechanism. Curr. Biol. *10*, 1311–1314.

Cox, J., and Mann, M. (2008). MaxQuant enables high peptide identification rates, individualized p.p.b.-range mass accuracies and proteome-wide protein quantification. Nat. Biotechnol. *26*, 1367–1372.

Cox, J., Neuhauser, N., Michalski, A., Scheltema, R.A., Olsen, J.V., and Mann, M. (2011). Andromeda: a peptide search engine integrated into the MaxQuant environment. J. Proteome Res. *10*, 1794–1805.

Dunn, J.G., Foo, C.K., Belletier, N.G., Gavis, E.R., and Weissman, J.S. (2013). Ribosome profiling reveals pervasive and regulated stop codon readthrough in Drosophila melanogaster. eLife *2*, e01179.

Edgar, B.A., Sprenger, F., Duronio, R.J., Leopold, P., and O'Farrell, P.H. (1994). Distinct molecular mechanism regulate cell cycle timing at successive stages of Drosophila embryogenesis. Genes Dev. *8*, 440–452.

Fenger, D.D., Carminati, J.L., Burney-Sigman, D.L., Kashevsky, H., Dines, J.L., Elfring, L.K., and Orr-Weaver, T.L. (2000). PAN GU: a protein kinase that

inhibits S phase and promotes mitosis in early Drosophila development. Development *127*, 4763–4774.

Gebauer, F., Xu, W., Cooper, G.M., and Richter, J.D. (1994). Translational control by cytoplasmic polyadenylation of c-mos mRNA is necessary for oocyte maturation in the mouse. EMBO J. *13*, 5712–5720.

Gentleman, R.C., Carey, V.J., Bates, D.M., Bolstad, B., Dettling, M., Dudoit, S., Ellis, B., Gautier, L., Ge, Y., Gentry, J., et al. (2004). Bioconductor: open software development for computational biology and bioinformatics. Genome Biol. *5*, R80.

Gildea, J.J., Lopez, R., and Shearn, A. (2000). A screen for new trithorax group genes identified little imaginal discs, the Drosophila melanogaster homologue of human retinoblastoma binding protein 2. Genetics *156*, 645–663.

Horner, V.L., and Wolfner, M.F. (2008a). Mechanical stimulation by osmotic and hydrostatic pressure activates Drosophila oocytes in vitro in a calcium-dependent manner. Dev. Biol. *316*, 100–109.

Horner, V.L., and Wolfner, M.F. (2008b). Transitioning from egg to embryo: triggers and mechanisms of egg activation. Dev. Dyn. *237*, 527–544.

Ingolia, N.T., Ghaemmaghami, S., Newman, J.R., and Weissman, J.S. (2009). Genome-wide analysis in vivo of translation with nucleotide resolution using ribosome profiling. Science *324*, 218–223.

Kashevsky, H., Wallace, J.A., Reed, B.H., Lai, C., Hayashi-Hagihara, A., and Orr-Weaver, T.L. (2002). The anaphase promoting complex/cyclosome is required during development for modified cell cycles. Proc. Natl. Acad. Sci. USA *99*, 11217–11222.

Kotani, T., Yasuda, K., Ota, R., and Yamashita, M. (2013). Cyclin B1 mRNA translation is temporally controlled through formation and disassembly of RNA granules. J. Cell Biol. *202*, 1041–1055.

Lee, L.A., Elfring, L.K., Bosco, G., and Orr-Weaver, T.L. (2001). A genetic screen for suppressors and enhancers of the Drosophila PAN GU cell cycle kinase identifies cyclin B as a target. Genetics *158*, 1545–1556.

Lee, L.A., Van Hoewyk, D., and Orr-Weaver, T.L. (2003). The Drosophila cell cycle kinase PAN GU forms an active complex with PLUTONIUM and GNU to regulate embryonic divisions. Genes Dev. *17*, 2979–2991.

Lloret-Llinares, M., Carré, C., Vaquero, A., de Olano, N., and Azorín, F. (2008). Characterization of *Drosophila melanogaster* JmjC+N histone demethylases. Nucleic Acids Res. *36*, 2852–2863.

Mermod, J.J., and Crippa, M. (1978). Variations in the amount of polysomes in mature oocytes of Drosophila melanogaster. Dev. Biol. *66*, 586–592.

Pesin, J.A., and Orr-Weaver, T.L. (2007). Developmental role and regulation of cortex, a meiosis-specific anaphase-promoting complex/cyclosome activator. PLoS Genet. *3*, e202.

Potireddy, S., Vassena, R., Patel, B.G., and Latham, K.E. (2006). Analysis of polysomal mRNA populations of mouse oocytes and zygotes: dynamic changes in maternal mRNA utilization and function. Dev. Biol. *298*, 155–166.

Qin, X., Ahn, S., Speed, T.P., and Rubin, G.M. (2007). Global analyses of mRNA translational control during early Drosophila embryogenesis. Genome Biol. *8*, R63.

Quintin, S., Mains, P.E., Zinke, A., and Hyman, A.A. (2003). The mbk-2 kinase is required for inactivation of MEI-1/katanin in the one-cell Caenorhabditis elegans embryo. EMBO Rep. *4*, 1175–1181.

Sagata, N. (1996). Meiotic metaphase arrest in animal oocytes: its mechanisms and biological significance. Trends Cell Biol. *6*, 22–28.

Sallés, F.J., Lieberfarb, M.E., Wreden, C., Gergen, J.P., and Strickland, S. (1994). Coordinate initiation of Drosophila development by regulated polyadenylation of maternal messenger RNAs. Science *266*, 1996–1999.

Schwanhäusser, B., Busse, D., Li, N., Dittmar, G., Schuchhardt, J., Wolf, J., Chen, W., and Selbach, M. (2011). Global quantification of mammalian gene expression control. Nature *473*, 337–342.

Secombe, J., Li, L., Carlos, L., and Eisenman, R.N. (2007). The Trithorax group protein Lid is a trimethyl histone H3K4 demethylase required for dMyc-induced cell growth. Genes Dev. *21*, 537–551.

Shamanski, F.L., and Orr-Weaver, T.L. (1991). The Drosophila *plutonium* and *pan gu* genes regulate entry into S phase at fertilization. Cell *66*, 1289–1300.

Stitzel, M.L., Pellettieri, J., and Seydoux, G. (2006). The *C. elegans* DYRK kinase MBK-2 marks oocyte proteins for degradation in response to meiotic maturation. Curr. Biol. *16*, 56–62.

Subtelny, A.O., Eichhorn, S.W., Chen, G.R., Sive, H., and Bartel, D.P. (2014). Poly(A)-tail profiling reveals an embryonic switch in translational control. Nature *508*, 66–71.

Swan, A., and Schüpbach, T. (2007). The Cdc20 (Fzy)/Cdh1-related protein, Cort, cooperates with Fzy in cyclin destruction and anaphase progression in meiosis I and II in Drosophila. Development *134*, 891–899.

Tadros, W., and Lipshitz, H.D. (2009). The maternal-to-zygotic transition: a play in two acts. Development *136*, 3033–3042.

Tadros, W., Houston, S.A., Bashirullah, A., Cooperstock, R.L., Semotok, J.L., Reed, B.H., and Lipshitz, H.D. (2003). Regulation of maternal transcript destabilization during egg activation in Drosophila. Genetics *164*, 989–1001.

Tadros, W., Goldman, A.L., Babak, T., Menzies, F., Vardy, L., Orr-Weaver, T., Hughes, T.R., Westwood, J.T., Smibert, C.A., and Lipshitz, H.D. (2007). SMAUG is a major regulator of maternal mRNA destabilization in Drosophila and its translation is activated by the PAN GU kinase. Dev. Cell *12*, 143–155.

Tay, J., Hodgman, R., and Richter, J.D. (2000). The control of cyclin B1 mRNA translation during mouse oocyte maturation. Dev. Biol. *221*, 1–9.

Vardy, L., and Orr-Weaver, T.L. (2007). The Drosophila PNG kinase complex regulates the translation of cyclin B. Dev. Cell *12*, 157–166.

Weil, T.T., Parton, R.M., Herpers, B., Soetaert, J., Veenendaal, T., Xanthakis, D., Dobbie, I.M., Halstead, J.M., Hayashi, R., Rabouille, C., and Davis, I. (2012). Drosophila patterning is established by differential association of mRNAs with P bodies. Nat. Cell Biol. *14*, 1305–1313.

Whitfield, Z.J., Chisholm, J., Hawley, R.S., and Orr-Weaver, T.L. (2013). A meiosis-specific form of the APC/C promotes the oocyte-to-embryo transition by decreasing levels of the Polo kinase inhibitor matrimony. PLoS Biol. *11*, e1001648.

Wiśniewski, J.R., Zougman, A., Nagaraj, N., and Mann, M. (2009). Universal sample preparation method for proteome analysis. Nat. Methods *6*, 359–362.

Young, R.A. (2011). Control of the embryonic stem cell state. Cell *144*, 940–954.

Zalokar, M. (1976). Autoradiographic study of protein and RNA formation during early development of Drosophila eggs. Dev. Biol. *49*, 425–437.